DOI: 10.1002/chem.200801555

Phase Behavior in Blends of Ethylene Oxide–Propylene Oxide Copolymer and Poly(ether sulfone) Studied by Modulated-Temperature DSC and NMR Relaxometry

Luk Van Lokeren,[a, b] Nicolaas-Alexander Gotzen,[a] Ronny Pieters,[a] Guy Van Assche,*[a] Monique Biesemans,[b] Rudolph Willem,[b] and Bruno Van Mele*[a]

Abstract: The state diagram of a blend consisting of a copolymer containing ethylene oxide and propylene oxide, P(EO-*ran*-PO), and poly(ether sulfone), PES, is constructed by using modulated-temperature differential scanning calorimetry (MTDSC), T_2 NMR relaxometry, and light scattering. The apparent heat capacity signal in MTDSC is used for the characterization of polymer miscibility and morphology development. T_2 NMR relaxometry is used to detect the onset of phase separation, which is in good agreement with the onset of phase separation in the apparent heat capacity from MTDSC and the cloud-point temperature as determined from light scattering. The coexistence curve can be constructed from T_2 values at various temperatures by using a few blends with well-chosen compositions. These T_2 values also allow the detection of the boundary between the demixing zones with and without interference of partial vitrification and are in good agreement with stepwise quasi-isothermal MTDSC heat capacity measurements. Important interphases are detected in the heterogeneous P(EO-*ran*-PO)/PES blends.

Keywords: differential scanning calorimetry · NMR relaxometry · phase diagrams · polymer blends · polymers

Introduction

The properties of partially miscible polymer blends are determined by their final morphology.[1,2] In the case of partially miscible polymer blends with a crystallizable component, for example, poly(ethylene oxide) (PEO), and a high-T_g component, poly(ether sulfone) (PES), the final state and properties of the blend are primarily governed by the kinetics of interfering transformations, including demixing, vitrification, and crystallization. In this study, modulated-temperature differential scanning calorimetry (MTDSC) and NMR T_2 relaxometry were used to monitor the phase behavior in partially miscible polymer blends.

MTDSC is an extension of conventional DSC, in which a sinusoidal perturbation is superimposed onto the underlying temperature program.[3–8] MTDSC allows for the simultaneous measurement of heat flow and heat capacity in both isothermal and non-isothermal conditions. This turned out to be very valuable for the study of rheological changes (vitrification) in reacting polymer systems.[6,9–11] The use of the temperature modulation for measuring the heat capacity also results in a superior performance for studying small heat capacity changes. Soon after its introduction, Hourston and co-workers exploited this advantage for studying miscibility and interphase formation in polymer blends through the study of their glass transition (T_g) behavior using the heat capacity and its temperature derivative.[6,12–15] It is generally recognized that the existence of a single, composition-dependent T_g in a blend indicates miscibility on a length scale of 10–30 nm,[16–18] while the presence of multiple T_gs indicates phase separation or partial miscibility of the blend components[19–21] on a similar length scale,[22,23] with each T_g

[a] L. Van Lokeren, N.-A. Gotzen, Dr. R. Pieters, Prof. G. Van Assche, Prof. B. Van Mele
Department of Materials and Chemistry
Research Unit Physical Chemistry
and Polymer Science (MACH/FYSC)
Vrije Universiteit Brussel, Pleinlaan 2
1050 Brussels (Belgium)
Fax: (+32) 2-629-32-78
E-mail: gvassche@vub.ac.be
bvmele@vub.ac.be

[b] L. Van Lokeren, Prof. M. Biesemans, Prof. R. Willem
Department of Materials and Chemistry
Research Unit High Resolution NMR Centre (MACH/HNMR)
Vrije Universiteit Brussel, Pleinlaan 2
1050 Brussels (Belgium)

reflecting a distinct segmental relaxation environment. The high sensitivity and good baseline performance of the MTDSC heat capacity signal renders the detection and quantification of T_g values and the associated increases in heat capacity ΔC_p (T_g) more reliable.

MTDSC is not only suitable for studying vitrification and glass transitions resulting from phase separation, but also for gaining a unique in situ insight into the kinetics of demixing and remixing in partially miscible polymer blends[24,25] and solutions.[26–29] During temperature-induced phase separation, mixing and/or demixing occur during each temperature modulation cycle and their heat effects contribute to the observed heat capacity signal, which is therefore termed an apparent heat capacity. Hence, isothermal demixing and remixing can be followed in real time by using quasi-isothermal heat capacity measurements. The observed time/temperature dependence of the apparent heat capacity under controlled conditions provides information on the kinetics and enables one to discriminate between fast molecular processes of mixing or demixing (nanoscale miscibility) and long-term evolutions at the macroscopic level, such as interphase or morphology development and partial vitrification. For polymer blends, this was illustrated for poly(ethylene oxide)/poly(ether sulfone) (PEO/PES) blends, showing the effects of blend composition and constituent molar mass on the demixing and remixing kinetics and the interrelation between both components.[24,25] This MTDSC methodology was extended to real-time observation of reaction-induced phase separation (RIPS). For low-T_g modifiers, the heat effects associated with phase separation contribute to the heat capacity signal, enabling the real-time measurement of the cloud point during RIPS.[30,31]

Herein, the methodology for studying the PEO/PES system by using MTDSC[24,25] is applied to a blend consisting of a random copolymer of ethylene oxide and propylene oxide, P(EO-*ran*-PO), and PES. The introduction of the propylene oxide comonomer reduces the miscibility and gives rise to an even smaller enthalpy of demixing for P(EO-*ran*-PO)/PES (less than 1 $J g^{-1}$) when compared to the PEO/PES system (less than 2 $J g^{-1}$). The P(EO-*ran*-PO)/PES system was selected because its lower critical solution temperature (LCST) behavior is similar to that of PEO/PES, but in a temperature range more suitable for a T_2 NMR relaxometry study (20–75 °C). The T_2 NMR relaxometry measurements will support and complement the MTDSC results. T_2 NMR relaxometry has proven its usefulness for studying multiphase systems.[32–37] The intensity decay of a pure component can usually be described as a single T_2 exponential decay, which can be used to characterize molecular and segmental mobility. Thus, for a pure polymer the monoexponential spin echo decay of amplitude $I(t)$, with amplitude I_0 at time t equal to zero and a single relaxation time T_2,[38] is described by Equation (1):

$$I(t) = I_0 \exp\left(-\frac{t}{T_2}\right) \quad (1)$$

For a multiphase system, the T_2 relaxation decay can be partitioned into discrete components, assigning higher T_2 values to more mobile phases and lower T_2 values to less mobile ones.[32] The various mechanisms inducing T_2 relaxation in spin $^1/_2$ systems all develop their own characteristic working distance. If domain sizes in heterogeneous systems are smaller than the working distance, relaxation of a nuclear spin in one phase will be induced by spins in the same phase as well as in the other phase. Under such conditions, finding a single T_2 value for all spins from both phases is likely. In contrast, if domain sizes are larger than the working distance, the relaxation of a nuclear spin in one phase will be induced only within that phase, resulting in a multiexponential decay for the whole system with, at best, a single exponential decay for each of its phases. Hence, if such a multiexponential decay is measured, it can be concluded that the heterogeneous system formed is very likely to display domain sizes larger than the working distance. For liquid-state ^{1}H NMR spectroscopy, relaxation induced by dipole–dipole interactions is the dominant relaxation mechanism and has a working distance of less than 1 nm.[39]

The power of the combination of NMR relaxometry and DSC was already shown for the investigation of different types of water in hydrogels (liquid-state NMR relaxometry)[36] and for probing the level of homogeneity in polymer blends characterized by one single T_g (solid-state NMR relaxometry).[40] In this study, MTDSC and liquid-state NMR relaxometry are combined to monitor the phase behavior in the partially miscible polymer blends, which provides novel insights into their morphology development and mobility of coexisting phases and interphases.

Results and Discussion

Construction of the state diagram of P(EO-ran-PO)/PES by using MTDSC: The state diagram of P(EO-*ran*-PO)/PES was constructed by using MTDSC. The important transition temperatures, for example, the glass transition temperature (T_g) and its width (ΔT_g), the melting temperature (T_m), and the cloud-point temperature (T_{cl}) can be obtained for each desired composition with a single MTDSC experiment by using the apparent heat capacity signal (C_p^{app}) as illustrated in Figure 1. T_g is taken at the inflection point in C_p^{app} (Figure 1, ◆ and ◇). Due to the high crystallization rate of P(EO-*ran*-PO), it is difficult to quench the blend to obtain a completely amorphous material. Furthermore, the cold crystallization starts immediately after partial devitrification of the quenched blend, as can be seen from the traces for the 90/10 and 80/20 blends in Figure 1, resulting in a more complicated and less reliable calculation of T_g and ΔT_g. For blends with a higher fraction of PES (35/65, 20/80 and 10/90 in Figure 1), the correct calculation of T_g and ΔT_g will be hampered by the interference of phase separation. Less reliable T_g values are indicated with an open diamond in Figure 1.

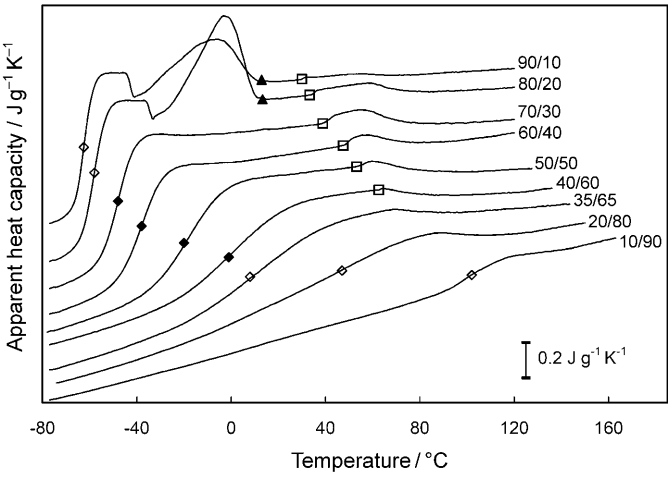

Figure 1. Non-isothermal MTDSC measurements: apparent heat capacity (C_p^{app}) versus temperature at a heating rate of 1 K min^{-1} for P(EO-*ran*-PO)/PES blends with the indicated compositions after quenching from the homogeneous melt: T_g (◆ and ◇, see text), T_m (▲) and T_{cl} (□).

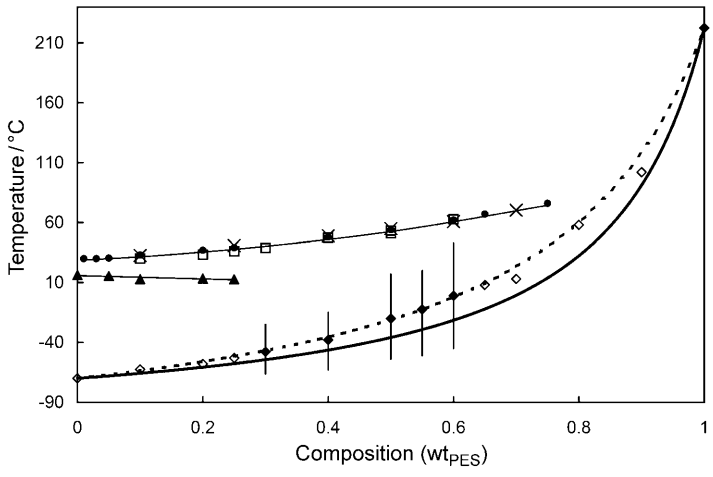

Figure 2. State diagram for P(EO-*ran*-PO)/PES: T_g (◆ and ◇, see text), ΔT_g (vertical bars), T_m (▲), T_{cl} as measured by MTDSC (□), by T_2 NMR relaxometry (×) and light scattering (●), and T_g-composition relations: Couchman[42] corresponding with $k=0.13$ (——) and Gordon–Taylor[41] with $k=0.18$ (-----).

The end set of the melting region is taken as T_m (Figure 1, ▲), whereas T_{cl} is taken as the onset of the apparent heat capacity (Figure 1, □). Below T_{cl} and above T_m, the heat capacity of the homogeneous P(EO-*ran*-PO)/PES melt only depends on the temperature and the blend composition. Under such conditions, the thermodynamic or baseline heat capacity (C_p^{base}) is measured. Upon phase separation, time- and temperature-dependent heat effects coupled with mixing/demixing occur during each modulation cycle and give rise to an excess heat capacity (C_p^{excess}). This C_p^{excess} term contributes to the measured apparent heat capacity signal, C_p^{app} [Eq. (2)].

$$C_p^{app}(T,t) = C_p^{base}(T) + C_p^{excess}(T,t) \quad (2)$$

For low amounts of the minor component, the heat of demixing is very small and the detection of the onset in the heat capacity signal is very difficult. Light scattering still allows for the detection of T_{cl} under these conditions.

All results from Figure 1 are combined in the state diagram of the P(EO-*ran*-PO)/PES system in Figure 2. Figure 2 also includes results obtained from T_2 NMR relaxometry and light scattering. For the latter, the onset of phase separation, detected through the onset of decrease in light transmittance, is taken as the cloud-point temperature T_{cl} (● in Figure 2). The determination of the cloud-point temperature by T_2 NMR relaxometry will be discussed later. The cloud-point temperatures obtained by using MTDSC are in good agreement with those obtained by light scattering and T_2 NMR relaxometry, as can be observed in Figure 2.

The state diagram evidences an LCST-type demixing behavior similar to the PEO/PES system.[24,25] The partial substitution of ethylene oxide with propylene oxide reduces the miscibility of the P(EO-*ran*-PO)/PES system when compared with PEO/PES: it shifts the demixing region to lower temperatures by about 45 °C. The heat of demixing of the P(EO-*ran*-PO)/PES system is smaller due to less interaction, which is at the origin of the reduced miscibility. The idea of a weaker interaction is supported by evaluating the composition dependence of T_g by using the Gordon–Taylor equation[41] with an adjustable parameter k taking into account the specific interactions. For the P(EO-*ran*-PO)/PES, a lower k parameter is found ($k=0.18$, dashed line in Figure 2) than for PEO/PES ($k=0.25$[24]), indicating less interactions in the former system. The Couchman approach for calculating the T_g of a homogeneous blend,[42] based on the T_g and ΔC_p at T_g of the pure components, does not take interactions into account and results in an even lower k parameter of 0.13.

The knowledge of T_g, T_m, and T_{cl} as a function of the blend composition allows the determination of four regions of interest: the (semicrystalline) glassy region below T_g, the semicrystalline region between T_g and T_m, the miscible homogeneous melt between T_m and T_{cl}, and the partially miscible heterogeneous region beyond T_{cl}. The T_2 NMR relaxometry study will focus on the latter two regions.

T_2 NMR relaxometry

Detection of the cloud-point temperature: In the homogeneous region, the blend displays a single T_2 relaxation time, which is observed as a linear decay of the logarithm of the reduced intensity versus time (Figure 3). Upon increasing the temperature from the homogeneous region, the blends start demixing owing to the LCST-type phase behavior evidenced in Figure 2. After phase separation, the coexisting phases have different compositions and thus their own characteristic molecular or segmental mobility, which is different from the one corresponding to the initial homogeneous composition. This results in a multiexponential T_2 relaxation

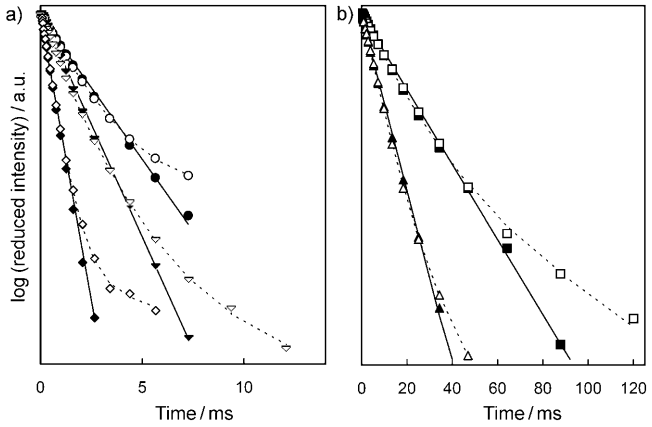

Figure 3. Detection of the cloud point as measured by NMR relaxometry for different compositions of P(EO-*ran*-PO)/PES: closed symbols for the highest temperature with monoexponential T_2 relaxation decay, open symbols for the lowest temperature with multiexponential T_2 relaxation decay: a) 60/40: ● (48.5 °C) and ○ (49.6 °C), 50/50: ▼ (54.3 °C) and ▽ (55.5 °C), 40/60: ◆ (59.1 °C) and ◇ (60.2 °C); b) 90/10: ■ (32.0 °C) and □ (33.1 °C), 75/25: ▲ (41.4 °C) and △ (42.6 °C).

decay in which each relaxation time characterizes one of the coexisting phases with a specific composition. Thus, upon phase separation, the relaxation decay changes from monoexponential to multiexponential, resulting in a nonlinear decay, as seen in Figure 3. The average of the highest temperature with a monoexponential decay, that is, the highest temperature at which the sample remains homogeneous, and the lowest temperature with a multiexponential decay, that is, the lowest temperature at which the sample is heterogeneous, is taken as the cloud-point temperature (T_{cl}) for that blend composition.

As shown in the state diagram for the P(EO-*ran*-PO)/PES system (Figure 2), there is a good correspondence between cloud-point temperatures determined by T_2 NMR relaxometry and those determined by MTDSC and light scattering, and this is true for all compositions. As the different techniques detect the onset of phase separation at different length scales, the good correspondence indicates a fast evolution of the domain size from less than one (NMR spectroscopy) to a few hundred (light scattering) nanometers.

Notwithstanding the satisfactory correspondence, the largest benefit of T_2 NMR relaxometry can be expected from the link between the relaxation time and the composition. For the heterogeneous blends, the T_2 relaxation times of each of the coexisting phases depend on each phase composition and the temperature. The purpose of monitoring the T_2 relaxation time dependence on composition and temperature for homogeneous blends is to establish the link between the relaxation times measured for heterogeneous blends and the composition of the coexisting phases.

Study of the homogeneous P(EO-ran-PO)/PES blends: The T_2 relaxation times of homogeneous blends were measured as a function of the temperature for blends with compositions ranging from pure P(EO-*ran*-PO) to a blend with PES (70 wt %).

For pure P(EO-*ran*-PO), T_2 relaxation times were measured for temperatures ranging from 20 to 75 °C. All spin echo decays were monoexponential. Furthermore, there is a satisfactory linear correlation between the logarithmic T_2 relaxation times and the reciprocal temperature (Figure 4), suggesting an Arrhenius correlation between T_2 and temperature. From molecular dynamics, it is well known that the mobility of molecules in liquids follows this type of temperature dependence.[43] Since T_2 relaxation times are related to molecular and segmental mobility, T_2 relaxation times can be expected to have a similar temperature dependence.

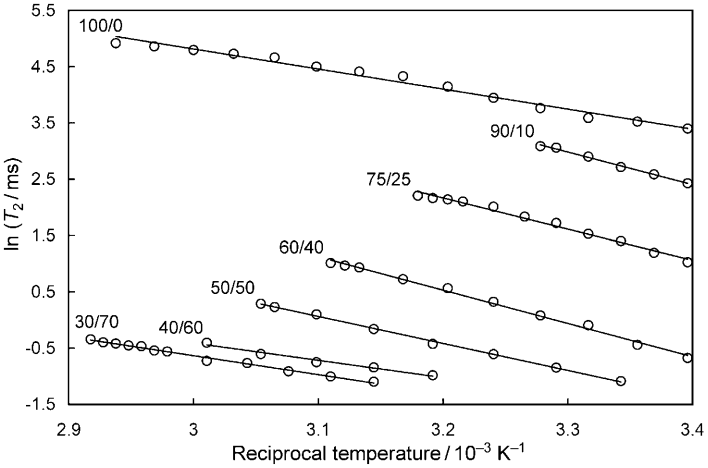

Figure 4. Arrhenius plot of the logarithmic T_2 relaxation time as a function of the reciprocal temperature for different compositions of P(EO-*ran*-PO)/PES in the homogeneous melt.

If polymers are mixed on a molecular scale, ideally all segments should have the same molecular environment and mobility, resulting in a single relaxation time. Although this simple view predicts a single relaxation time for homogeneous blends, all data points of the intensity decay were fitted toward a multiexponential decay to allow a priori for multiple relaxation times in the data analysis. Nevertheless, all multiexponential fittings for homogeneous blends resulted in a monoexponential decay with a single T_2 relaxation time (not shown). For all compositions, the obtained T_2 relaxation times show an Arrhenius temperature dependence, as shown in Figure 4. Higher PES contents result in a lower T_2 relaxation time in the blend, owing to the lower mobility of this high T_g component than pure P(EO-*ran*-PO). For the highest PES contents (30/70 and 40/60), the blends are partially vitrified and highly viscous at the lowest temperatures. As long as the T_2 relaxation time is above 0.2 ms, it can be determined by using liquid-state T_2 NMR relaxometry.

There is an exponential correlation between T_2 and the blend composition at different temperatures (Figure 5), however, within a limited composition range from roughly 0.1 to 0.5 weight fraction (indicated with a solid trendline). By interpolation on Figure 5, the blend composition at a

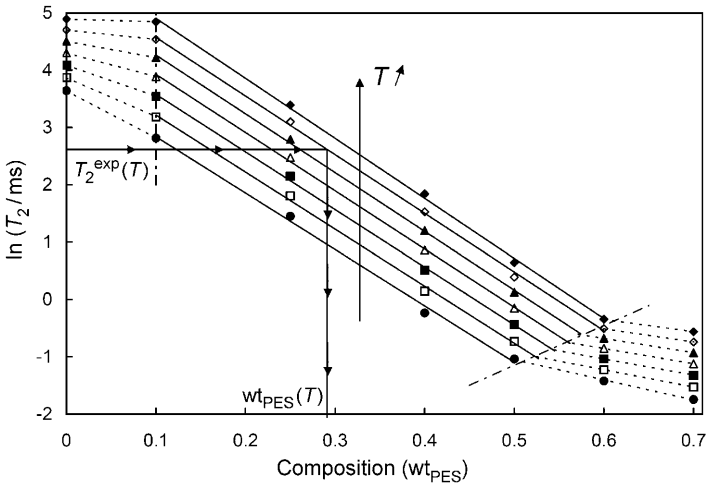

Figure 5. Logarithmic T_2 relaxation time as a function of composition for P(EO-*ran*-PO)/PES blends at different temperatures, calculated by using the inter- and extrapolated values from Figure 4: 27.2 °C (●), 33.1 °C (□), 39.0 °C (■), 44.9 °C (△), 50.8 °C (▲), 56.6 °C (◇), and 62.5 °C (◆). The estimation of the composition of a phase based on its T_2 relaxation time measured at a certain temperature (here 56.6 °C) is illustrated.

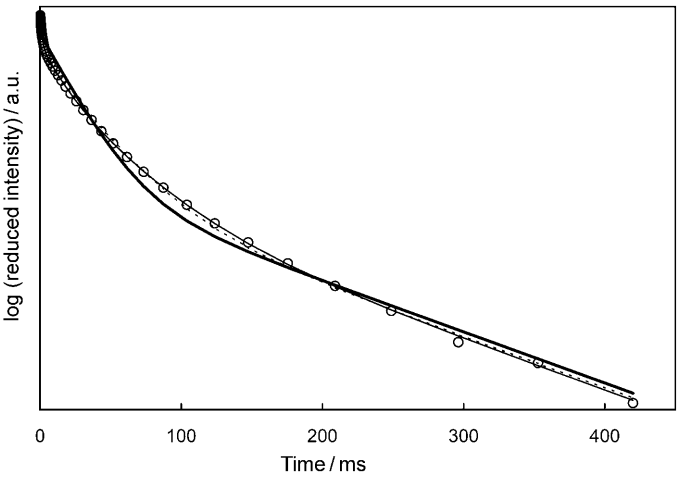

Figure 6. T_2 NMR relaxation decay for a P(EO-*ran*-PO)/PES 60/40 at 56.7 °C at equilibrium, fitted with a sum of two (——), three (-----) and four (——) discrete exponentials.

given temperature can be determined from its observed T_2 relaxation time. The exponential correlation from Figure 4, which was used to determine the blend composition at a given temperature in the homogeneous region from its T_2 relaxation time by interpolation, will also be used in the heterogeneous region by simultaneous extrapolation and interpolation.

Study of the heterogeneous P(EO-ran-PO)/PES blends: Heterogeneous P(EO-*ran*-PO)/PES blends clearly exhibit a multiexponential T_2 relaxation decay, as shown in Figure 3 (open symbols). From the state diagram (Figure 2), one would expect that the T_2 relaxation decays in the partially miscible heterogeneous region consist of the two relaxation times corresponding to a P(EO-*ran*-PO)-rich phase with a higher T_2 relaxation time than the homogeneous phase, and a P(EO-*ran*-PO)-poor phase with a lower T_2 relaxation time, with compositions corresponding to the coexistence curve.[44] Actually, the P(EO-*ran*-PO)-rich phase consists of almost pure P(EO-*ran*-PO), as indicated by the state diagram (Figure 2). When fitting the relaxation decay with a discrete distribution of T_2 relaxation times, the two expected T_2 relaxation times are found. They do not suffice, however, to describe the measured relaxation decay. At least one or two additional T_2 relaxation times are needed, the best fit being obtained for a total of four T_2 relaxation times (Figure 6). For the phase-separated polymer blends, one could expect a concentration gradient, or an interphase, to be present between the phases; a common feature in heterogeneous multicomponent systems.[12–14] This interphase would be characterized by a distribution of relaxation times. Therefore, all intensity decays were fitted not only by a discrete but also by a continuous distribution of relaxation times, as implemented in the CONTIN algorithm by Provencher.[45,46] As shown in Figure 7, the fitting with a continuous distribution results in four relaxation peaks, with T_2 relaxation times and fractions that are very close to those obtained through the fitting with discrete relaxation times. The two extra phases, corresponding to the two extra T_2 relaxation times needed in addition to those corresponding to the expected coexisting phases, have compositions in between the compositions of the cloud-point curve and can be attributed to interphases.[6,12–14]

Whereas the composition of each phase is estimated from its T_2 relaxation time, the weight fraction of each phase can be estimated from the initial amplitude of the spin echo decay of the corresponding T_2 relaxation time. For Figure 7, this results in two interphases corresponding to about 50 %

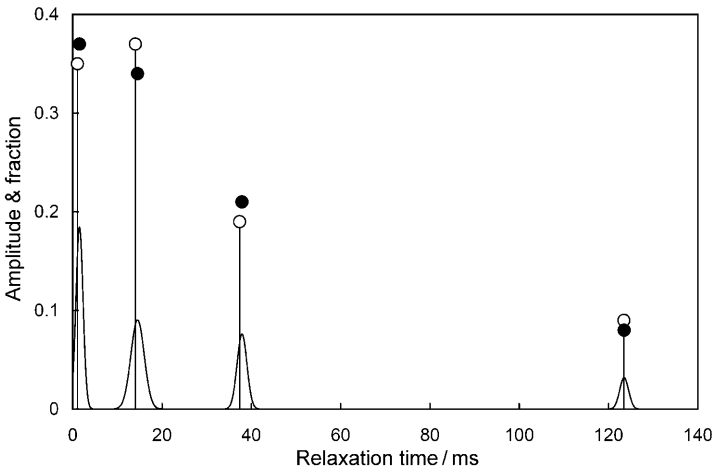

Figure 7. Amplitude versus relaxation time distribution for a P(EO-*ran*-PO)/PES 60/40 at 56.7 °C at equilibrium, showing the continuous composition distribution obtained by the CONTIN algorithm (solid peaks) and the discrete distribution with four relaxation times (○). The height of the symbols corresponds to the fractional contributions of the four peaks of the continuous distribution (●) and the four relaxation times of the discrete distribution (○), respectively.

by weight of the polymer blend. This important interphase is probably linked to a fine phase-separated morphology and a large contact area between the phases. This is in agreement with MTDSC, the reversible demixing-remixing on the timescale of the modulation, as observed by the heat effect in C_p^{app}, can only be achieved if the corresponding mass transport phenomena occur over a large interfacial contact area.

Constructing the coexistence curve by using T_2 *NMR relaxometry*: As described above, the multiexponential relaxation decay in the partially miscible heterogeneous region contains the relaxation times corresponding to the compositions of the coexistence curve. By performing a stepwise isothermal T_2 NMR relaxometry experiment, that is, increasing the temperature in steps of only a few K and measuring the T_2 relaxation decay after each temperature increase, enables one to construct a section of the coexistence curve. As the phase compositions are formed instantaneously, the first relaxation decay at each temperature suffices to construct a complete phase diagram with a single stepwise isothermal measurement. To capture the minimum of the LCST, one should use a blend with a composition corresponding to the minimum of the cloud-point curve. However, in the case of P(EO-*ran*-PO)/PES, the cloud-point curve is very asymmetrical and thus the minimum of its cloud-point curve corresponds with almost pure P(EO-*ran*-PO) (Figure 2). Therefore, four P(EO-*ran*-PO)-rich blends with compositions ranging from P(EO-*ran*-PO)/PES 90/10 up to 50/50 were selected for constructing the coexistence curve. Note that in this particular blend, the coexistence curve matches the experimental cloud-point temperatures as detected by MTDSC and light scattering (Figure 8). Although this approach permits the construction of a section of the coexistence curve by using a single sample with a well-chosen starting composition, it also implies the knowledge of the dependence of the T_2 relaxation times on the composition at different temperatures. However, in addition to the coexistence curve, this method also gives information about the amount and the composition of the interphase(s), as discussed previously.

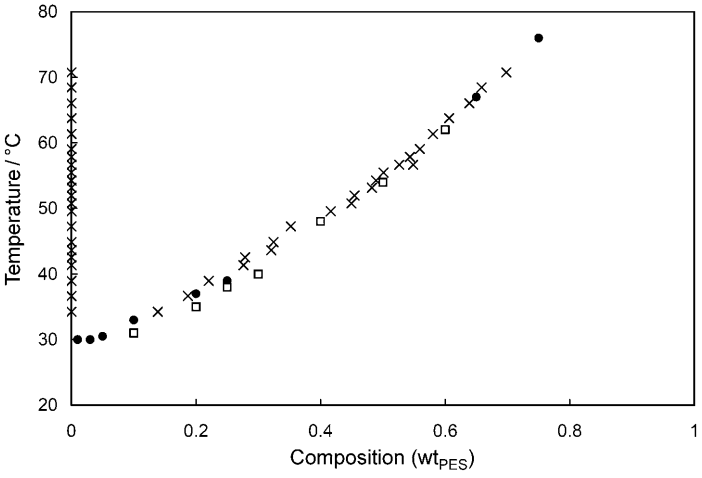

Figure 8. Coexistence curve for P(EO-*ran*-PO)/PES as constructed by a stepwise isothermal T_2 NMR relaxometry experiment (×), starting from four blends with compositions 90/10, 75/25, 60/40, and 50/50. Cloud points as detected by MTDSC (□) and light scattering (●).

Influence of partial vitrification during phase separation: During phase separation of a polymer blend or polymer solution, (partial) vitrification of a phase occurs if the T_g of that phase approaches the temperature at which phase separation occurs.[24,25,28,29]

Referring to the phase diagram (Figure 2), it is observed that at weight fractions of PES above 0.7, the end set of the glass transition interferes with the cloud-point curve. For temperatures above this intersection, an increase in temperature will result in the partial vitrification of the high-T_g PES-rich phase. Therefore, the partially miscible region can be subdivided in two regions: a demixing zone without interference of partial vitrification (zone I) and a demixing zone with interference of partial vitrification (zone II).

MTDSC enables one to detect vitrification during phase separation in stepwise quasi-isothermal, heat capacity (C_p) measurements, as shown for the PEO/PES system.[24] The same stepwise quasi-isothermal MTDSC approach was used for the P(EO-*ran*-PO)/PES system (Figure 9). After reaching a stable C_p^{app} (● in Figure 9), corresponding to the final state at the chosen temperature, a stepwise increase of 1 K was applied. Below the cloud point, all quasi-isothermal C_p^{app} levels coincide with the C_p^{base} measured during heating at 1 K min^{-1} (zone 0). Above the cloud point, heat effects coupled with mixing/demixing during one modulation cycle contribute to the heat capacity signal. Note that the C_p^{app} evolution measured at 1 K min^{-1} does not coincide with the final C_p^{app} levels, which illustrates the time dependence of C_p^{excess} in the demixing zone, as in the PEO/PES system.[24] The decrease of the final C_p^{app} levels below the extrapolated C_p^{base}

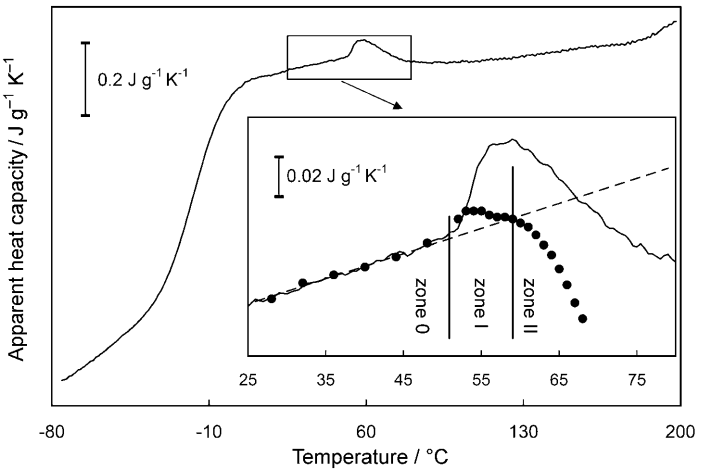

Figure 9. Stepwise quasi-isothermal MTDSC experiment for a P(EO-*ran*-PO)/PES 50/50 blend, with the final C_p^{app} level (●) indicated at each temperature superimposed on C_p^{app} measured at 1 K min^{-1} (——); extrapolation of the baseline heat capacity from the homogeneous melt (-----).

from the miscible melt (dashed line in Figure 9) at about 60 °C, indicates the occurrence of partial vitrification of the high-T_g PES-rich phase. Note that the actual temperature range in which vitrification occurs depends on the heating rate used, shifting to lower temperatures at slower rates (compare stepwise quasi-isothermal to $1\,K\,min^{-1}$ in Figure 9).

The (partial) vitrification of the high-T_g phase is also apparent in the T_2 NMR relaxometry results. Liquid-state T_2 NMR relaxometry allows the detection of T_2 relaxation times above the T_2 detection limit of about 0.2 ms. For materials with a T_2 relaxation time below this detection limit, the relaxation decay is too fast and the material will not be visible. Hence partial vitrification of one of the coexisting phases in a demixed polymer blend leads to the partial apparent "disappearance" of this phase when using liquid-state T_2 NMR relaxometry.

In the case of P(EO-*ran*-PO)/PES blends, a part of the high-T_g PES-rich phase will no longer be observed, and the remaining average detectable composition becomes richer in P(EO-*ran*-PO). In Figure 10, a stepwise isothermal T_2 NMR relaxometry measurement is shown for a P(EO-*ran*-PO)/PES 50/50 blend. The average detectable composition is depicted as a function of time and temperature. In zone 0 (miscible melt) and in zone I (phase separation without interference of vitrification), the average visible composition equals the homogeneous start composition ($w_{PES}=0.5$). From 61 °C onwards and over a range of about 5 °C, the average composition becomes richer in P(EO-*ran*-PO), implying partial vitrification of the PES-rich phase (zone II), in good agreement with the MTDSC results (compare Figures 9 and 10).

Conclusions

T_2 NMR relaxometry and MTDSC prove to be powerful and complementary tools for studying partially miscible polymer blends, such as P(EO-*ran*-PO)/PES. By using MTDSC, a state diagram was constructed, evidencing LCST behavior with a strongly asymmetric cloud-point curve, with the critical composition very close to the pure low-T_g P(EO-*ran*-PO). At weight fractions of high-T_g PES of 70 wt % and above, the high temperature end set of the glass transition interferes with the cloud-point curve, resulting in a partial vitrification of the PES-rich phase at temperatures above the intersection (60 °C).

The onset of phase separation as detected by T_2 NMR relaxometry through the change from a monoexponential to a multiexponential decay is in accordance with the MTDSC and light-scattering results. This good agreement indicates that the morphology evolves quickly from the molecular scale (T_2 NMR relaxometry), through the nm scale (MTDSC), to the sub-μm scale (light scattering). Through calibration with data from homogeneous blends, the compositions corresponding to the observed relaxation times can be obtained. Exploiting this methodology, a section of the coexistence curve is constructed by using stepwise, quasi-isothermal measurements for a single blend composition. In the present system, the coexistence curve coincides with the cloud-point curve. The fact that both the cloud-point curve (onset of phase separation) and the coexistence curve can be determined by T_2 NMR relaxometry, might offer interesting opportunities for studying systems in which the two curves do not coincide.[47] Moreover, by using T_2 NMR relaxometry, the presence of one or two interphases could be detected and their composition and weight fraction could be determined, which gave interesting information on the phase structure developed.

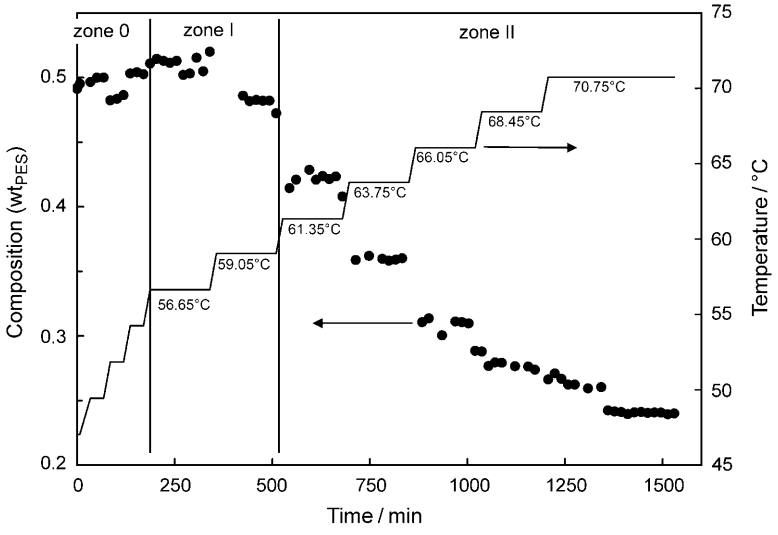

Figure 10. Stepwise isothermal T_2 NMR relaxometry measurement for a P(EO-*ran*-PO)/PES 50/50 blend depicting the average detected composition (●) as a function of temperature and time.

Experimental Section

Materials: The random copolymer of ethylene oxide and propylene oxide, P(EO-*ran*-PO), with a number average molar mass of $2500\,g\,mol^{-1}$ was supplied by Aldrich. The copolymer contains 75 % ethylene oxide and 25 % propylene oxide and is terminated by hydroxyl groups. This copolymer is semicrystalline with a melting temperature of about 15 °C. The glass transition temperature, T_g, and the increment in heat capacity at T_g, ΔC_p, measured by using MTDSC amount to −70 °C and approximately $0.95\,J\,g^{-1}\,K^{-1}$, respectively.

Poly(ether sulfone) or poly(1,4-phenylene ether sulfone), PES, with a viscosity average molar mass of $20000\,g\,mol^{-1}$ was supplied by Aldrich. The T_g and ΔC_p at T_g of PES (totally amorphous) measured by using MTDSC equal 222.5 °C and $0.21\,J\,g^{-1}\,K^{-1}$, respectively.

P(EO-ran-PO)/PES blend preparation: Blends with compositions ranging from pure P(EO-*ran*-PO) to pure PES were obtained by preparing 10 % (w/v) solutions of both components in *N*,*N*-dimethylformamide, fol-

lowed by the removal of the solvent under vacuum at 30 °C. The blends were additionally dried overnight at a temperature just below the cloud-point temperature of the blend estimated from previous results. The composition of the blends is expressed as the weight ratio of P(EO-*ran*-PO)/PES.

Techniques

Liquid-state NMR relaxometry: The proton transverse relaxation time (T_2) measurements were performed on a Bruker Avance II NMR spectrometer operating at 500.13 MHz, using a TBI probe head equipped with a *z*-gradient coil. All spectra were recorded over the temperature range from 20 to 75 °C. The temperature, controlled by a Bruker BVT 3000 unit, was calibrated by using neat ethylene glycol as described in reference [48]. The temperature accuracy is ±0.5 °C. The T_2 times were measured by using the Carr–Purcell–Meiboom–Gill (CPMG) sequence until the signal intensity dropped below 1 % of its value.

MTDSC: MTDSC measurements were performed on a TA Instruments 2920 DSC with MDSC option and on a TA Instruments Q1000 equipped with a RCS or LNCS cooling system, respectively. Helium or nitrogen was used as a purge gas (25 mL min^{-1}). Indium and cyclohexane were used for temperature calibration. The former was also used for enthalpy calibration. Heat capacity calibration was performed with poly(methyl methacrylate) (PMMA; supplied by Acros) by using the heat capacity difference between two temperatures,[49] one above and one below the glass transition temperature of PMMA, to make sure that heat capacity changes were adequately measured.

Standard modulation conditions used in the experiments are an amplitude of 1 K (2920 DSC) or 0.5 K (Q1000 DSC) and a period, *p*, of 60 s. Non-isothermal experiments were performed at an underlying heating rate of 1 K min^{-1}.

Samples were pretreated under vacuum at a temperature of 5 K below the expected cloud point of the blend, prior to the introduction into the DSC. Samples of 5 to 10 mg were introduced in TA Instruments hermetic pans. These crucibles were perforated to ensure an inert atmosphere around the sample, reducing degradation of P(EO-*ran*-PO) at higher temperatures. The drying step was repeated for a couple of hours to ensure the removal of all solvent and moisture.

Light scattering: Cloud points were detected by measuring the light transmitted through thin samples between glass slides in a Mettler Toledo FP82HT hot stage equipped with a photodetector. A Spectratech optical microscope was used with a magnification of four and a light source operating with visible light (between 400 and 800 nm with an average value of 600 nm). All samples were heated at a rate of 1 K min^{-1} to reduce thermal lag in the sample and to allow comparison with MTDSC measurements at the same underlying heating rate. A nitrogen purge was applied to avoid degradation of P(EO-*ran*-PO) at higher temperatures. The onset of the decrease in the transmitted light intensity was chosen as the cloud-point temperature.[24]

Acknowledgements

The financial support by the fund of Scientific Research Flanders (Belgium) (FWO) (Grants G.0469.06 & G.0064.07, a postdoctoral fellowship (G.V.A.), a PhD fellowship (N.A.G.)) and the Research Council (Onderzoeksraad) of the Vrije Universiteit Brussel (Concerted Research Action, Grant GOA31) to R.W. and L.V.L. is gratefully acknowledged.

[1] R. E. Prud'homme, *Polym. Eng. Sci.* **1982**, *22*, 90–95.
[2] C. Koning, M. van Duin, C. Pagnoulle, R. Jerome, *Prog. Polym. Sci.* **1998**, *23*, 707–757.
[3] P. S. Gill, S. Sauerbrunn, M. Reading, *J. Therm. Anal.* **1993**, *40*, 931–939.
[4] M. Reading, D. Elliott, V. Hill, *J. Therm. Anal.* **1993**, *40*, 949–955.
[5] M. Reading, A. Luget, R. Wilson, *Thermochim. Acta* **1994**, *238*, 295–307.
[6] *Modulated-Temperature Differential Scanning Calorimetry: Theoretical and Practical Applications in Polymer Characterisation (Hot Topics in Thermal Analysis and Calorimetry)*, 1st ed. (Eds.: M. Reading, D. J. Hourston), Springer, Dordrecht, The Netherlands, **2006**.
[7] K. J. Jones, I. Kinshott, M. Reading, A. A. Lacey, C. Nikolopoulos, H. M. Pollock, *Thermochim. Acta* **1997**, *305*, 187–199.
[8] B. Wunderlich, *J. Therm. Anal. Calorim.* **2006**, *85*, 179–187.
[9] G. Van Assche, A. Van Hemelrijck, H. Rahier, B. Van Mele, *Thermochim. Acta* **1995**, *268*, 121–142.
[10] S. Swier, B. Van Mele, *Thermochim. Acta* **1999**, *330*, 175–187.
[11] G. Van Assche, S. Swier, B. Van Mele, *Thermochim. Acta* **2002**, *388*, 327–341.
[12] M. Song, A. Hammiche, H. M. Pollock, D. J. Hourston, M. Reading, *Polymer* **1995**, *36*, 3313–3316.
[13] M. Song, A. Hammiche, H. M. Pollock, D. J. Hourston, M. Reading, *Polymer* **1996**, *37*, 5661–5665.
[14] D. J. Hourston, M. Song, A. Hammiche, H. M. Pollock, M. Reading, *Polymer* **1997**, *38*, 1–7.
[15] Y. Miwa, K. Usami, Y. Katsuhiro, M. Sakaguchi, M. Sakai, S. Shimada, *Macromolecules* **2005**, *38*, 2355–2361.
[16] L. A. Utracki, *Polymer Blends Handbook*, Kluwer Academic, Dordrecht, The Netherlands, **2002**.
[17] Q. R. Huang, H. C. Kim, E. Huang, D. Mecerreyes, J. L. Hedrick, W. Volksen, C. W. Frank, R. D. Miller, *Macromolecules* **2003**, *36*, 7661–7671.
[18] A. Nathanson, *Polym. Eng. Sci.* **1992**, *32*, 1711–1715.
[19] A. R. Shultz, B. M. Gendron, *J. Appl. Polym. Sci.* **1972**, *16*, 461–471.
[20] E. J. Beckman, F. E. Karasz, R. S. Porter, W. J. Macknight, J. Vanhunsel, R. Koningsveld, *Macromolecules* **1989**, *22*, 1193–1194.
[21] T. Inoue, *Prog. Polym. Sci.* **1995**, *20*, 119–153.
[22] H. W. Kammer, J. Kressler, C. Kummerloewe, *Adv. Polym. Sci.* **1993**, *106*, 31–86.
[23] P. S. O. Patricio, J. A. de Sales, G. G. Silva, D. Windmöller, J. C. Machado, *J. Membr. Sci.* **2006**, *271*, 177–185.
[24] S. Swier, R. Pieters, B. Van Mele, *Polymer* **2002**, *43*, 3611–3620.
[25] G. Dreezen, G. Groeninckx, S. Swier, B. Van Mele, *Polymer* **2001**, *42*, 1449–1459.
[26] S. Swier, K. Van Durme, B. Van Mele, *J. Polym. Sci. Part B: Polym. Phys.* **2003**, *41*, 1824–1836.
[27] K. Van Durme, G. Van Assche, B. Van Mele, *Macromolecules* **2004**, *37*, 9596–9605.
[28] K. Van Durme, S. Verbrugghe, F. E. Du Prez, B. Van Mele, *Macromolecules* **2004**, *37*, 1054–1061.
[29] K. Van Durme, G. Van Assche, V. Aseyev, J. Raula, H. Tenhu, B. Van Mele, *Macromolecules* **2007**, *40*, 3765–3772.
[30] S. Swier, B. Van Mele, *Polymer* **2003**, *44*, 2689–2699.
[31] S. Swier, B. Van Mele, *Macromol. Symp.* **2003**, *198*, 363–375.
[32] E. Von Meerwall, T. Stone, *J. Polym. Sci. Part B: Polym. Phys.* **1989**, *27*, 503–522.
[33] G. Iannacchione, E. Von Meerwall, *J. Polym. Sci. Part B: Polym. Phys.* **1991**, *29*, 659–668.
[34] D. Mahoney, E. Von Meerwall, *J. Polym. Sci. Part B: Polym. Phys.* **1993**, *31*, 1029–1039.
[35] C. N. Barros, E. P. G. Arêas, E. N. Figueiredo, J. A. G. Arêas, *Colloids Surf. B* **2006**, 48, 119–127.
[36] M. Carenza, G. Cojazzi, B. Bracci, L. Lendinara, L. Vitali, M. Zincani, M. Yoshida, R. Katakai, E. Takacs, O. Z. Higa, F. Martellini, *Radiat. Phys. Chem.* **1999**, *55*, 209–218.
[37] R. Mens, P. Adriaensens, L. Lutsen, A. Swinnen, S. Bertho, B. Ruttens, J. D'Haen, J. Manca, T. Cleij, D. Vanderzande, J. Gelan, *J. Polym. Sci. Part B: Polym. Phys.* **2008**, *46*, 138–145.
[38] F. A. Bovey, P. A. Mirau, *NMR of Polymers*, Academic Press, London, UK, **1996**.
[39] B. Cowan, *Nuclear Magnetic Resonance and Relaxation*, University Press, Cambridge, **1997**, pp. 207–253.
[40] L. L. Chang, E. M. Woo, *J. Polym. Sci. Part B: Polym. Phys.* **2003**, *41*, 772–784.
[41] M. Gordon, J. S. Taylor, *J. Appl. Chem.* **1952**, *2*, 493–500.

[42] P. R. Couchman, F. E. Karasz, *Macromolecules* **1978**, *11*, 117–119.
[43] P. W. Atkins, *Physical Chemistry, Molecules in motion*, Oxford University Press, Oxford, **2000**.
[44] It should be noted that the compositions of the coexistence curve can differ from those of the cloud-point curve (see R. Koningsveld, *Discuss. Faraday Soc.* **1970**, 49, 144–161 or reference [47]).
[45] S. W. Provencher, *Comput. Phys. Commun.* **1982**, *27*, 213–217.
[46] S. W. Provencher, *Comput. Phys. Commun.* **1982**, *27*, 229–242.
[47] R. Koningsveld, W. H. Stockmayer, E. Nies, *Polymer phase diagrams*, Oxford University Press, Oxford, **2001**.
[48] T. D. Claridge, *High-Resolution NMR Techniques in Organic Chemistry*, Pergamon, Oxford, **1999**.
[49] U. Gaur, B. Wunderlich, *J. Phys. Chem. Ref. Data* **1982**, *11*, 313–325.

Received: July 30, 2008
Published online: December 16, 2008

